Hindawi
International Journal of Chemical Engineering
Volume 2018, Article ID 4715629, 9 pages
https://doi.org/10.1155/2018/4715629

Research Article

Catalytic Activity of a Composition Based on Strontium Bismuthate and Bismuth Carbonate at the Exposure to the Light of the Visible Range

K. S. Makarevich, A. V. Zaitsev, O. I. Kaminsky, E. A. Kirichenko, and I. A. Astapov

Institute of Materials Khabarovsk Scientific Center, Far Eastern Branch of the Russian Academy of Sciences, Khabarovsk, Russia

Correspondence should be addressed to O. I. Kaminsky; kamin_div0@mail.ru

Received 13 April 2018; Revised 26 July 2018; Accepted 6 August 2018; Published 10 September 2018

Academic Editor: Gianluca Di Profio

This paper presents the results pertaining to studying the properties of the photocatalytically active composition of strontium bismuthate $SrBi_{2.70}O_{5.05}$, $SrBi_{2.90}O_{5.35}$, and $SrBi_{3.25}O_{5.88}$ and bismuth carbonate $(BiO)_2CO_3$ in molar ratios 1/0.67, 1/0.56, and 1/0.37, respectively. These compositions are obtained through pyrolytic synthesis from organic precursor complexes of strontium and bismuth with sorbitol. It has been established that the synthesised powder materials absorb the light of the visible range up to 500 nm owing to the presence of a narrow-gap semiconductor strontium bismuthate. The presence of a wide-band semiconductor $(BiO)_2CO_3$ ensures an effective separation of electron-hole pairs. The diffuse reflection spectra (DRS) of compositions differ from the analogous spectra of a mechanical mixture of these semiconductor phases with the same composition, which allows one to assume the heterostructural structure of the semiconductor system. The same heterostructure is confirmed by the results of mapping. Catalytic particles that are synthesised at a temperature of 500°C containing 27 mass% $(BiO)_2CO_3$ (corresponding to $SrBi_{2.9}O_{5.35}/(BiO)_2CO_3 = 1/0.56$) have the greatest activity with respect to the photodecomposition of methylene blue (MB). The possibility of controlling the optical properties and photocatalytic activity of the composition is depicted due to the joint formation of the strontium bismuthate phase and the bismuth carbonate phase.

1. Introduction

Organic compounds are often the primary toxic components of wastewater from various origins. Photocatalysis became a promising technology for their purification after the publication of one of the pioneering works in this regard, which was written by Frank and Bard in 1977 [1]. On the other hand, studies concerning photocatalytically active semiconductors began to develop intensively after the publication of the well-known work of Fujishima and Honda [2], which lead to the publication of a large series of articles by various authors dedicated to obtaining hydrogen from water using light energy. Both the aforementioned processes are based on the phenomenon of photolysis of water on the surface of a semiconductor under the action of light. As a result, strong oxidising agents, such as atomic oxygen, free hydroxide radicals, hydrogen peroxide, to name a few, are produced with the capacity of ensuring deep oxidation of organic compounds. The undoubted advantage of this method concerning organic removal is the lack of regular costs for additional chemical reagents. Consequently, the method of photocatalytic purification has found wide application, from the final stage of the treatment of drinking water at water intake stations to the sewage treatment conducted in industries such as oil refining, paint and varnish, and textile.

The search for new catalytically active systems, capable of photolysis of water under the influence of sunlight, has been conducted for the purpose of creating compositions based on narrow-gap semiconductors having an absorption region in the visible spectral range [3, 4]. In particular, they include

semiconductors based on transition metal oxides. However, photocatalysts with this composition have a significant disadvantage that is associated with the toxicity of the heavy metals included in them (e.g., Cd and Pb) [5–7], which makes it impossible to utilise such substances for water purification. It is known that bismuth is an exception in terms of being a toxicological hazard among heavy metals. Its toxicity is so minute that bismuth compounds have been found, for instance, to be widely used in pharmacology as antacid agents for oral administration [8, 9]. This is owing to the fact that mobile cationic forms of bismuth are not formed in alkaline, neutral, and weakly acidic media. Thus, during the purification of water, its saturation with regard to bismuth is excluded. Among bismuth compounds, high catalytic activity comparable to anatase shows the presence of carbonate $(BiO)_2CO_3$. However, the region of its intrinsic absorption lies in the UV range of the spectrum. To sensitise $(BiO)_2CO_3$ to visible light, it is doped with nitrogen [10, 11]. Other bismuth compounds, such as the narrow-band semiconductor $CaBi_6O_{10}$, do not require the use of additives, since they are characterised by intrinsic absorption in the visible spectral range [12, 13]. However, they are less effective with regard to the photodecomposition of organic compounds. One way to increase the reactivity of narrow-band semiconductors is to create heterostructural composites with wide-gap semiconductors.

As a rule, two-phase compositions are synthesised in two stages: first, the main component is obtained, after which a second component is formed on its surface. In this method of production, it is difficult to achieve a uniform mutual distribution of semiconductors in the concerned volume. Therefore, in our study, we employed the previously developed pyrolytic synthesis method based on bismuth complexes with sorbitol [14], which simultaneously produces a composition of two semiconductors. As a wide-gap semiconductor, $(BiO)_2CO_3$ was formed in the composition. Moreover, the absorption of visible light was achieved owing to the introduction of strontium bismuthate, which occupies a central position in the solid solutions presented in the $SrO\text{-}Bi_2O_3$ diagram [15]. The purpose of this study was to create and study the properties of $SrBi_xO_y/(BiO)_2CO_3$ compounds of various compositions, depending on the synthesis conditions. Furthermore, it purposes to reveal the phase composition of the catalyst, providing the greatest photocatalytic activity of the composition during the decomposition of the organic dye.

2. Experiment

$SrBi_4O_7$ and several compositions based on it were obtained through a modified method of pyrolytic synthesis. Previously, we employed this method to obtain $CaBi_6O_{10}$. Strontium nitrate $Sr(NO_3)_2$ (ACROS), bismuth nitrate pentahydrate $Bi(NO_3)_3{\cdot}5H_2O$ (ACROS), and sorbitol $C_6H_{14}O_6$ served as precursors for the synthesis of composites based on $SrBi_xO_y$.

The amount of sorbitol in the precursor mixture's composition increased by 1.5 times in comparison to [16], which allowed the amount of CO_2 and $(BiO)_2CO_3$, together with $SrBi_xO_y$, to increase. The mixture of $Sr(NO_3)_2$, $Bi(NO_3)_3{\cdot}5H_2O$, and sorbitol (Sr : Bi = 1 : 4 molar ratio) was grinded in mortar. The grinded mixture spontaneously formed a transparent viscous solution due to the hydrated water of nitrates. Pyrolysis of the precursor mixture was conducted at 180°C in the air. Subsequently, the pyrolyzed mixture was heated to temperatures of 300, 400, 500, 600, and 700°C and was held isothermally for 24 hours. The obtained $SrBi_xO_y/(BiO)_2CO_3$ compositions have been designated as SBC-X, where X signifies the synthesis temperature. The concentration of $(BiO)_2CO_3$ in the obtained samples was measured by dissolving the sample in 10% HCl solution. Subsequently, the amount of CO_2 released was estimated by making use of a $Ba(OH)_2$ solution. In addition, Brunauer–Emmett–Teller (BET) specific surface area of the samples was measured via N_2 adsorption at 77 K by using Sorbi 4.1. analyser. The crystal in a phase of the samples was identified through X-ray diffraction by utilising a DRON-7 diffractometer with CuKα ($\lambda = 1.5406$ Å) as the radiation source, which operated at 40 kV and 40 mA. Moreover, the UV and visible diffuse reflectance spectra were conducted on a MDR-41 spectrophotometer system equipped with an integrating sphere attachment, with $BaSO_4$ as the background. Surface morphology and distribution of particles were studied by LEO 1430VP SEM, by employing an accelerating voltage of 15 kV.

Furthermore, photocatalytic experiments were performed using an automated photometric unit [17]. Photocatalytic activities of the samples SBC-X were evaluated through the degradation of methylene blue solution ($1.2\ mg{\cdot}L^{-1}$, 350 mL) under different light irradiations discharge lamp Aqua Arc Osram, Sylvania (250 W, continuous spectrum $\lambda = 380$–850 nm). Mass of photocatalyst sample is 200 mg. The spectrum of the lamp was similar to the spectral distribution of the radiation intensity with regard to sunlight. To cut out the UV range, a filter ($\lambda > 380$ nm) was employed. During the irradiation, the solution was stirred using a IKA RO10 magnetic stirrer. The temperature of the photocatalytic system was maintained at 25°C by utilising the water-cooling thermostat (Julabo F25-ED).

3. Results and Discussion

The study of the process of phase formation in the system under investigation upon its heating yielded the following results. The composition at 300–400°C consists of three phases. In the temperature range, the composition at 500–600°C has a two-phase composition. At 700°C, the composition becomes single-phase. This can be seen from XRD (Figure 1). On the XRD patterns of these samples, there are pronounced reflections belonging to $\alpha\text{-}Bi_2O_3$ and $(BiO)_2CO_3$. In addition, there are peaks corresponding to a solid solution of the $SrO\text{-}Bi_2O_3$ system with stoichiometry similar to $SrBi_3O_{5.5}$ (ICDD-45-609). Furthermore, analysis of the XRD patterns of sample SBC-400 revealed that the concentration of Bi_2O_3 is reduced in this regard, which indicates the introduction of Bi_2O_3 into a solid solution of strontium bismuthate. In this sample, $(BiO)_2CO_3$ has not decomposed yet. The intensity of its diffraction peaks does not change in comparison to SBC-300. On the XRD pattern of sample SBC-500, an increase in the intensity of the reflex

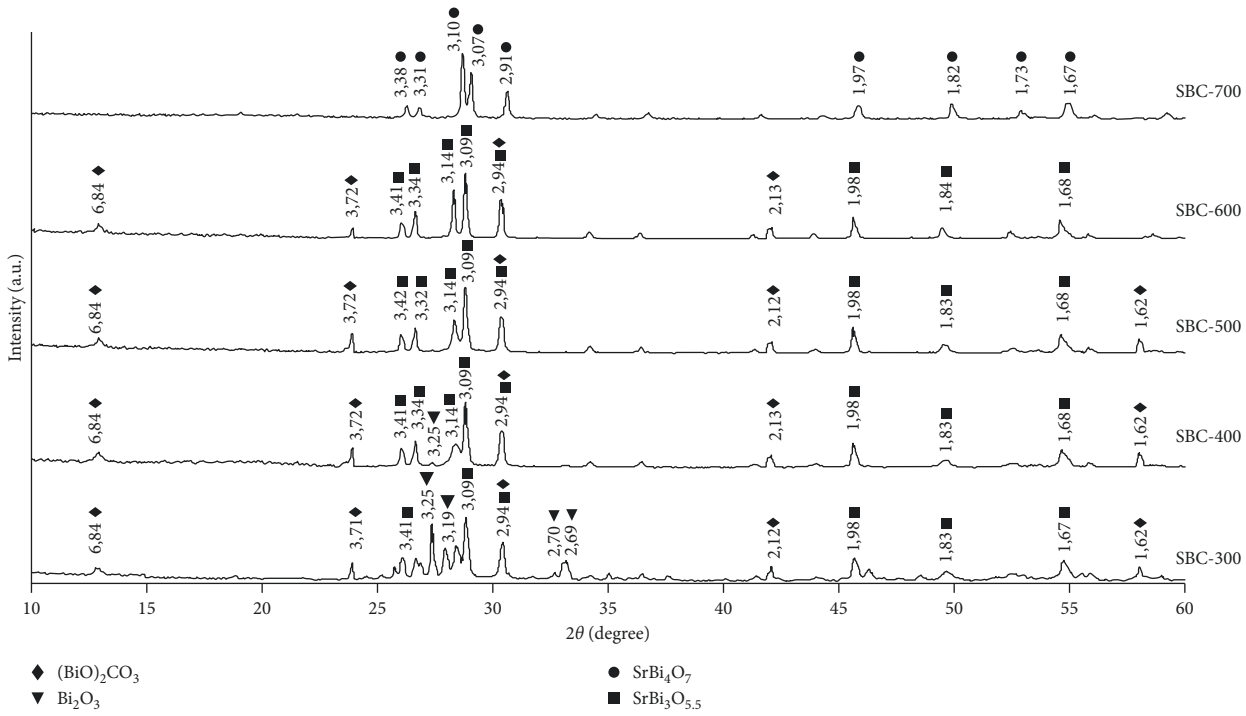

Figure 1: XRD patterns of samples obtained at different synthesis temperatures.

3.14 Å is observed. This demonstrates that the solid solution of strontium bismuthate continues to be formed through the incorporation of unreacted bismuth oxide. At temperatures above 600°C, $(BiO)_2CO_3$ is partially decomposed, and the intensity of its reflexes decreases. The bismuth oxide formed during the decomposition of $(BiO)_2CO_3$ enters a solid solution based on strontium bismuthate. This process is characterised by an increase in the intensity of the reflex 3.14 Å. At a temperature of 700°C, the process concerning the formation of a solid solution of strontium bismuthate ends. This is confirmed by the displacement of all the peaks in the region of large angles and through a change in the ratio of the two primary phase reflexes (3.11 and 3.07 Å) of strontium bismuthate. Consequently, the diffractogram assumes the form that is typical of a solid solution of strontium bismuthate with stoichiometry close to $SrBi_4O_7$. Based on the results of XRD, the strontium carbonate phase was not found.

Chemical analysis revealed that the concentration of carbonates in the samples obtained at 300°C to 400°C is approximately the same and equal to 29–32 wt%. The content $(BiO)_2CO_3$ in the sample SBC-500 is about 27% and 18% in the SBC-600 composition.

The results of the mapping show that there are areas containing predominantly strontium and having insignificant quantity of carbon. Comparing with XRD data, these areas were identifiable, like the phase of strontium bismuthate. The remaining surface of the sample contains bismuth, oxygen, and carbon, but so does insignificant quantity of strontium and is identifiable as bismuth carbonate. As can be seen from Figure 2, the bismuth carbonate phase has high roughness, while the bismuth-strontium phase is represented by a smooth surface. The formation of such a structure is possible due to the epitaxial growth in the process of joint synthesis of both semiconductors that make up the composition. The synthesized compositions are represented by two main particle fractions, where the smaller one ($(BiO)_2CO_3$) has a nanometer size range, and the large ones have a strontium-bismuthate phase with particle sizes of about 1.5–3.5 μm that form agglomerates. The average size of the agglomerates is in the range of 20–50 μm.

By conducting a comparative analysis of XRD data and chemical analysis, it can be assumed that the obtained compositions have the following content (Table 1). As it is commonly known [15], the phase diagram of SrO-Bi_2O_3 rather has a wide range of solid solutions. According to refined data [18], a solid solution is formed under the condition that the Sr : Bi atomic ratio is in the range from 1 : 2.5 to 1 : 7.5, meaning that it corresponds to compounds with stoichiometry from $SrBi_{2.5}O_{4.75}$ to $SrBi_{7.5}O_{12.25}$. According to XRD data, the strontium bismuthate formed in the compositions is most close to with Sr : Bi 1 : 3 stoichiometry $SrBi_3O_{5.5}$ (ICDD-45-609) and, consequently, is a representative of these series of solid solutions. The reflexes characteristic of this strontium bismuthate were identified for the samples SBC-400, SBC-500, and SBC-500. However, a more accurate identification of the stoichiometry of strontium bismuthate obtained from XRD data is not possible, since the samples contain $(BiO)_2CO_3$, whose main reflexes are superposition or close to the reflections of strontium bismuthate from the above series of solid solutions. In order to identify more accurately the stoichiometry of the formed bismuth phases, we additionally carried out a chemical analysis that made it possible to determine the content of $(BiO)_2CO_3$ in the samples. Further, a simple calculation was carried out, based on the following facts: firstly, the total atomic Sr : Bi

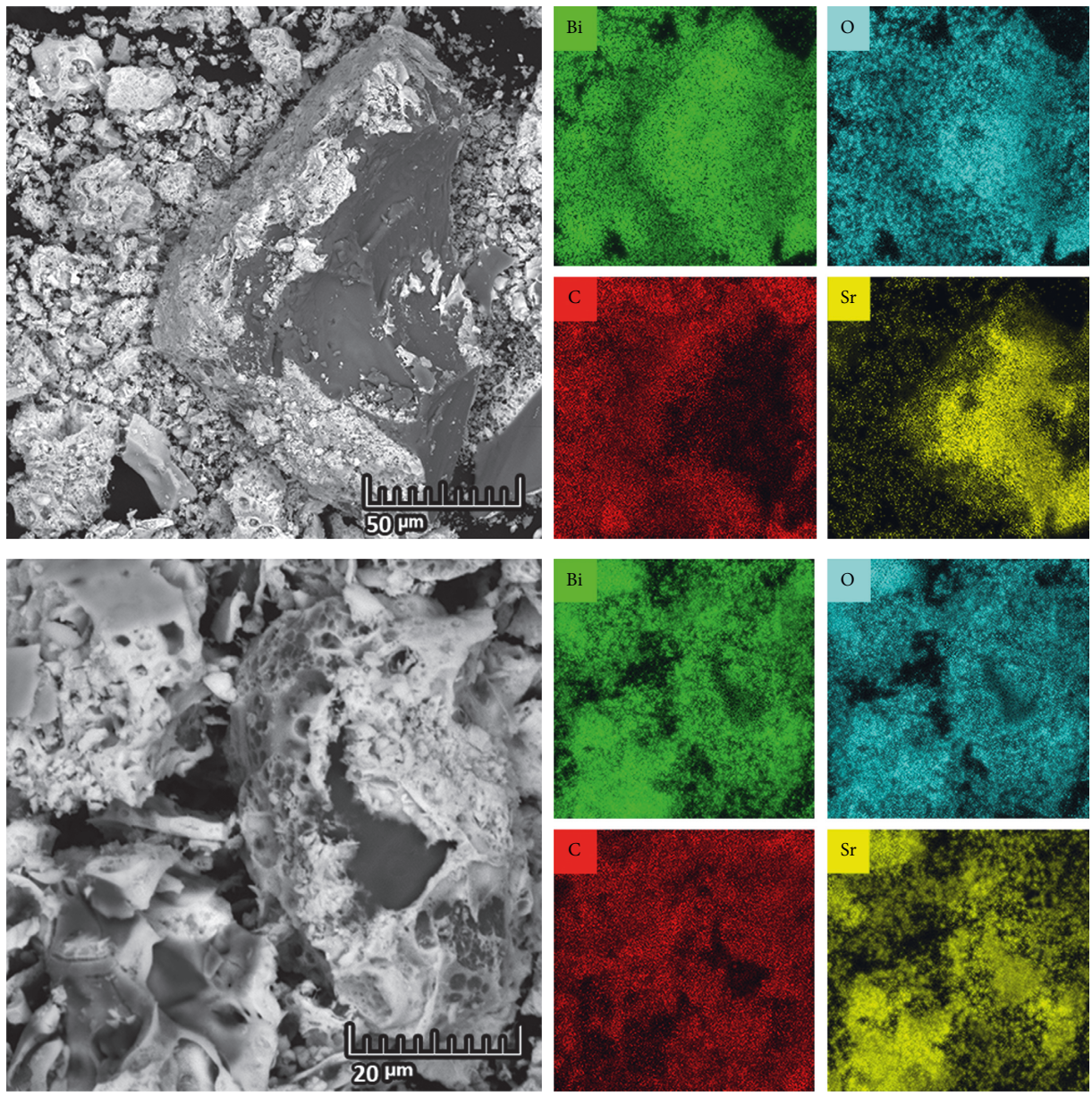

Figure 2: SEM images of composed SBC-500 and results of mapping.

Table 1: The content of semiconductor phases in the obtained compositions.

Photocatalysts	Total atomic ratio Sr : Bi in the compositions	Weight content $(BiO)_2CO_3$ (%)	Photocatalysts $SrBi_xO_y/(BiO)_2CO_3$	
			Element stoichiometry in phases	Molar ratio of phases in the compositions
SBC-400	1 : 4	32	$SrBi_{2.70}O_{5.05}/(BiO)_2CO_3$	1/0.67
SBC-500	1 : 4	27	$SrBi_{2.90}O_{5.35}/(BiO)_2CO_3$	1/0.56
SBC-600	1 : 4	18	$SrBi_{3.25}O_{5.88}/(BiO)_2CO_3$	1/0.37
$SrBi_4O_7$	1 : 4	0	$SrBi_4O_7$	1/0

ratio in all the obtained compositions was set equal to 1 : 4 during the synthesis, secondly, the samples of SBC-400, SBC-500, and SBC-600 are two-phase, and thirdly, the content of $(BiO)_2CO_3$ is accurately known from the chemical analysis. Therefore, by knowing the share of bismuth that went to the formation $(BiO)_2CO_3$, it is possible to calculate the share of bismuth that went to the formation of strontium bismuthate, i.e., to clarify the stoichiometry of Sr : Bi in the solid solution formed (Table 1). The data obtained in this way are in good agreement with the results of XRD. The adjusted Sr : Bi ratio is actually close to 1 : 3 and is 1/2.7, 1/2.9, and 1/3.25 for the samples

of SBC-400, SBC-500, and SBC-600, respectively. The composition SBC-300 (based on XRD data) is three-phase, since it contains, in addition to the two phases described above, also Bi_2O_3. Accordingly, the use of the above sequence of calculations in relation to it will not be correct. For this reason, the sample SBC-300 is not included in Table 1. A more detailed study of it was not the purpose of this paper, since the compositions formed by bismuth oxide and alkaline earth metal bismuth were previously investigated by many authors, for example, in [10–12]; in addition, the sample SBC-300 did not show a high catalytic activity.

The composition SBC-400 has the greatest specific surface area of 3.5 m^2/g, according to BET analysis (Table 2). Increasing the synthesis temperature from 400°C to 600°C leads to the fact that the specific surface area of the samples is reduced to 3.0 m^2/g. This is probably due to the gradual decomposition of the carbonate phase $(BiO)_2CO_3$ and the coarsening of the particles belonging to the formed solid solution of strontium bismuthate. When the carbonate is completely decomposed, the single-phase $SrBi_4O_7$ sample obtained at 700°C has a specific surface area of 2.4 m^2/g. This is comparable to the specific area of pure α-Bi_2O_3 (2.2 m^2/g), which is obtained in the same manner. Hence, the presence of a carbonate phase contributes to the formation of a more developed surface in two-phase compositions.

Based on the DRS for each synthesised composition, $SrBi_4O_7$, and $(BiO)_2CO_3$, the Kubelka–Munk function $F(R) = 0.5(1–R)^2/(R–1)$ was calculated, where R represents the reflection coefficient. The widths of the band gap are determined from the point of intersection of the function graph's linear section $(F(R)\ h\nu)^{1/2}$ with the axis of abscissae: photon energy $h\nu$ (Figure 3). According to the concerned estimates, the width of the forbidden band of $SrBi_4O_7$ and $(BiO)_2CO_3$ was $E_g = 2.50$ eV and 3.38 eV, respectively. Moreover, analysis of the dependencies $(F(R)\ h\nu)^{1/2}$ for the compositions SBC-500 and SBC-600 showed that they can be divided into two linear Sections *I* and *II* (Figure 3). They are a superposition of the graphs of two semiconductors that constitute the composition. Section *I* corresponds to bismuth carbonate, whereas section *II* corresponds to strontium bismuthate. As the synthesis temperature increases, section *I* decreases, and section *II*, respectively, increases due to the increase in the proportion of strontium bismuthate in the solid solution. Comparing the analogous curves concerning a mechanical mixture of 73% $SrBi_4O_7$ + 27% $(BiO)_2CO_3$, one can note that there is a marked difference between them. Investigation of optical properties has shown that the spectra of DRS compositions do not signify a simple superposition of the semiconductor phases that form them and differ from the spectra of a mechanical mixture with the same composition. Their distinctive feature is the characteristic absorption region in the range of 200–270 nm, which is absent on the individual phases' spectra of the composition's constituents and on the spectrum of a simple mechanical mixture identical to the composition of the relevant composition.

Studying the photocatalytic activity of synthesised materials demonstrated that their use makes it possible for one to increase the decomposition rate of methylene blue upon irradiation with visible light. Kinetic dependences of the change in the concentration of organic dye, in the presence of the synthesised compositions SBC 300–700, $SrBi_4O_7$, and α-Bi_2O_3, have been depicted in Figure 4. The single-phase samples of $SrBi_4O_7$ and α-Bi_2O_3 possess the lowest catalytic activity. Moreover, the activity of $SrBi_4O_7$ is moderately higher than that of bismuth oxide. This is owing to the wider absorption region of $SrBi_4O_7$. The catalytic activity of biphasic compositions in all cases was observed to be higher. We attribute this result to the cocatalytic effect of the interaction of the $SrBi_xO_y/(BiO)_2CO_3$ phases forming the composition. Its occurrence is possible due to the heterostructural nature of the structure of the composition. This is confirmed by the data of the SEM mapping of the images given earlier. The possibility of epitaxial growth is also indicated by similar X-ray structural parameters of the obtained strontium bismuthate and bismuth carbonate. To test this assumption, a mechanical mixture was prepared from the separately obtained $SrBi_4O_7$ and $(BiO)_2CO_3$ phases and an identical SBC-500 sample, exhibiting the greatest catalytic activity. The catalytic activity of the prepared mixture (Figure 4) showed an intermediate value between the activities of its constituent phases and is inferior to the activity of any of the obtained compositions, including SBC-500. Therefore, the joint-phase formation during synthesis is a prerequisite for the efficient operation of the photocatalytic composition.

The sample synthesised at 500°C exhibits greatest catalytic activity. This is probably related to the formation of the required amount of strontium bismuthate, which sensitises the system to visible light. On the contrary, $(BiO)_2CO_3$ is retained in sufficient amount (27%) for the efficient functioning of the catalyst. When its quantity is reduced to 18%, the efficiency of the SBC-600 catalyst decreases. In sample SBS-400 (32%-$(BiO)_2CO_3$), there is not enough strontium bismuthate, and hence the catalyst is not capable of absorbing the energy of visible light. The reaction rate constant (k) was determined by determining the parameters of the linear regression equations for the $(C_t/C_0) = f(t)$ dependencies. The obtained values of k have been presented in Table 2. It is known that the samples under study have different specific surface areas. For a correct comparison of the catalytic activity, the rate constant $k_s \cdot 10^{-4}$, normalised to the specific surface, was calculated (Table 2). With an increase in the synthesis temperature of the samples, their catalytic activity increases and becomes greatest for the SBC-500 composition ($k_s = 4.69$). A further increase in temperature at first leads to a decrease in the k_s constant (4.33)

Table 2: The catalytic activity of the resulting compositions and single-phase photocatalysts.

Sample	Specific surface area, S (m^2/g)	Reaction rate constant, $k \cdot 10^{-3}$ (min^{-1})	Specific reaction rate constant, $k_s \cdot 10^{-4}$ ($g \cdot min^{-1} \cdot m^{-2}$)
α-Bi_2O_3	2.1	4.0	1.90
SBC-300	3.2	9.0	2.81
SBC-400	3.5	1.3	3.71
SBC-500	3.2	1.5	4.69
SBC-600	3.0	1.3	4.33
$SrBi_4O_7$	2.4	8.0	3.33

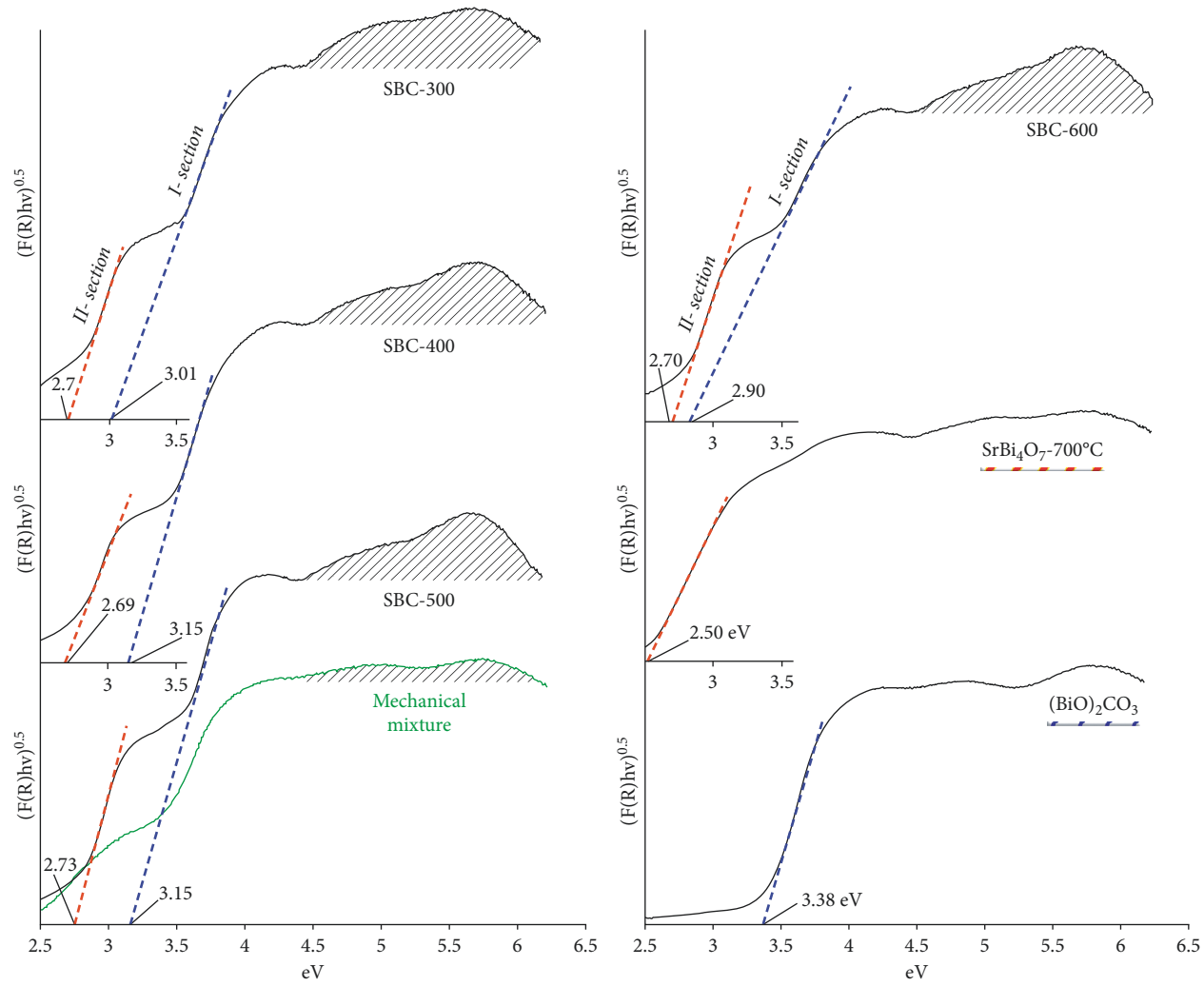

Figure 3: Dependences $(F(R)h\nu)^{1/2}$ of single-phase samples of $SrBi_4O_7$ and $(BiO)_2CO_3$ and the compositions SBC-300, SBC-400, SBC-500, and SBC-600 and their mechanical mixture of 73% $SrBi_4O_7$ + 27% $(BiO)_2CO_3$ from photon energy.

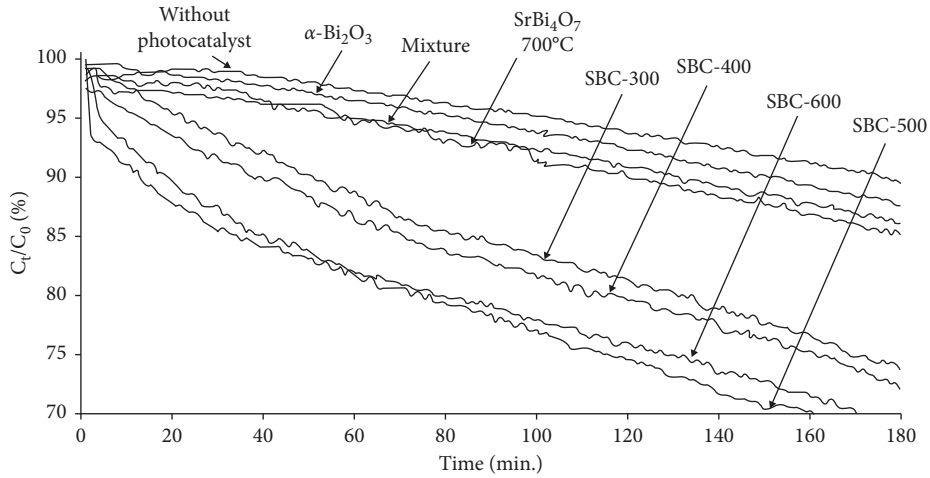

Figure 4: Photocatalytic decomposition curves of MB under irradiation with visible light in the presence of SBC-300, SBC-400, SBC-500, and SBC-600 and single-phase samples of $SrBi_4O_7$, and α-Bi_2O_3 and a mechanical mixture of 73% $SrBi_4O_7$ + 27% $(BiO)_2CO_3$.

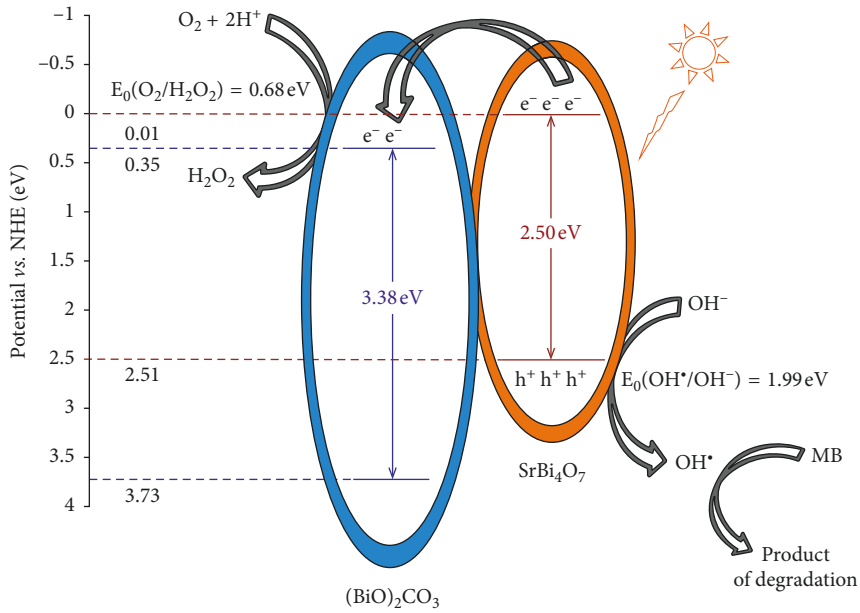

FIGURE 5: The possible degradation mechanism of MB over the prepared composites.

for the SBC-600 sample. Subsequently, it exhibits a significant drop in k_s (3.33) at a temperature of 700°C, when the composition becomes single-phase. A comparative analysis of the obtained data k_s shows that the high catalytic activity of the compositions in comparison with monophases and a mechanical mixture is primarily due to the heterostructural phase content, and not only to the developed surface.

4. Discussion

The results of this study obtained can be explained by considering the cocatalytic effect of the different phases in the composition of $SrBi_xO_y/(BiO)_2CO_3$. The formation of such a structure is possible owing to the epitaxial growth in the process of joint synthesis of both semiconductors constituting the composition. Moreover, the possibility of epitaxial growth is also indicated by similar X-ray structural parameters of the obtained strontium bismuthate and bismuth carbonate. The catalytic activity of the mixture of 73% $SrBi_4O_7$ + 27% $(BiO)_2CO_3$ (Figure 4) demonstrated an intermediate value between the activities of its constituent phases, which are inferior to the activity of any of the resulting compositions, including SBC-500. Consequently, the formation of heterostructural phases in the synthesis process increases the efficiency of the photocatalytic composition. Furthermore, values pertaining to the boundaries of the valence band (VB) and the conduction band (CB) of $SrBi_4O_7$ and $(BiO)_2CO_3$ compounds were calculated by employing the following equations [19]:

$$E_{VB} = XE - E^e + 0.5E_g, \quad (1)$$

$$E_{CB} = XE - E^e - 0.5E_g, \quad (2)$$

where XE signifies the absolute electronegativity of the semiconductor, which is calculated as the geometric mean of the absolute electronegativity of the atoms forming it (the XE values for $SrBi_4O_7$ and $(BiO)_2CO_3$ are 5.76 eV and 6.54 eV, resp.); E^e represents the absolute potential of the standard hydrogen electrode (4.5 eV); E_{VB} denotes the VB edge potential (the VB potential); E_{CB} signifies the CB edge potential (the CB value); E_g represents the energy of a semiconductor's band gap, which is experimentally obtained from an analysis of the spectra of DRS. According to the calculations, the upper boundary of the VB zone and the lower CB boundary for $SrBi_4O_7$ are 2.51 eV and 0.01 eV, respectively, whereas for $(BiO)_2CO_3$, it was 3.73 and 0.35 eV. The band structure of the obtained samples can be depicted in the form of the circuit as shown in Figure 5.

Exposure to visible light results in the generation of electron-hole pairs only in the narrowband semiconductor $SrBi_4O_7$, since $(BiO)_2CO_3$ does not possess the ability to utilise the energy of the spectrum's visible part (Figure 5). The energies of CB and VB $SrBi_4O_7$ are higher than that of $(BiO)_2CO_3$. Moreover, the transition of photogenerated electrons from the conduction band of $SrBi_4O_7$ to the conduction band $(BiO)_2CO_3$ is energetically favorable. Consequently, electrons accumulate in the conduction band of a wide-gap semiconductor, whereas holes remain in the valence band of $SrBi_4O_7$, which leads to a spatial separation of the charge carriers. Thus, the lifetime of charge carriers is significantly increased, which contributes to formation of a more efficient flow concerning photolysis of water. The value of the CB potential of both semiconductors (0.01 and 0.35 eV) is lower than the O_2/H_2O_2 potential, which ensures the reduction of dissolved oxygen to hydrogen peroxide:

$$O_2 + 2H^+ + 2e^- = H_2O_2; \quad E_0 = +0.682 \text{ eV} \quad (3)$$

Subsequently, peroxide is able to recombine with hydroxide radicals, which are active agents for the destruction of organic compounds. In addition, the formation of

hydroxide radicals also occurs in a narrow-gap semiconductor, since the value of VB for $SrBi_4O_7$ (2.51 eV) is more positive in comparison to the oxidation potential of hydroxide ions in a photohole:

$$HO^- + h^+ = HO^\bullet; \quad E_0 = +1.99 \text{ eV} \tag{4}$$

Photoholes in VB $SrBi_4O_7$, in turn, can directly oxidise MB when absorbing dye molecules on the semiconductor surface.

5. Conclusions

(i) Through the method pertaining to oxidative pyrolysis of complexes of the corresponding metals with sorbitol, it is depicted that it is possible to obtain a composition based on strontium bismuthate and bismuth carbonate. The photocatalytic activity of such a composition under the action of visible light is higher than that of a mechanical mixture of the same composition, the α-Bi_2O_3 and $SrBi_4O_7$ phases. The greatest catalytic activity is possessed by compositions that are obtained at 500 to 600°C containing 73–82 mass.%, $SrBi_xO_y$, and 27–18 mass.%, $(BiO)_2CO_3$; it corresponds of strontium bismuthate $SrBi_{2.9}O_{5.35}$, $SrBi_{3.25}O_{5.88}$, and bismuth carbonate $(BiO)_2CO_3$ in molar ratios 1/0.56; 1/0.37, respectively.

(ii) Investigation of optical properties has shown that the spectra of DRS compositions do not signify a simple superposition of the semiconductor phases that form them and differ from the spectra of a mechanical mixture with the same composition. Their distinctive feature is the characteristic absorption region in the range of 200–270 nm, which is absent on the individual phases' spectra of the composition's constituents and on the spectrum of a simple mechanical mixture identical to the composition of the relevant composition.

(iii) Analysis of DRS and the results of mapping suggest heterostructural nature of the compositions. The formation of such a structure is possible due to epitaxial growth, bismuth carbonate on strontium bismuthate during the synthesis of $SrBi_xO_y/(BiO)_2CO_3$.

(iv) The mechanism concerning the photocatalytic activity of the semiconductor phases forming studied the composition is explained on the basis of the band structure's analysis.

(v) The results of the work present the prospects for creating environmentally safe and efficient photocatalysts based on bismuth compounds that are sensitive to visible light irradiation

Data Availability

The data used to support the findings of this study are available from the corresponding author upon request.

Conflicts of Interest

The authors declare that they have no conflicts of interest.

References

[1] S. N. Frank and A. J. Bard, "Semiconductor electrodes. Photoassisted oxidations and photoelectrosynthesis at polycrystalline titanium dioxide electrodes," *Journal of the American Chemical Society*, vol. 99, no. 14, pp. 4667–4675, 1977.

[2] A. Fujishima and K. Honda, "Electrochemical photolysis of water at a semiconductor electrode," *Nature*, vol. 238, no. 5358, pp. 37–45, 1972.

[3] W. Mekprasart and W. Pecharapa, "Synthesis and characterization of nitrogen-doped TiO_2 and its photo-catalytic activity enhancement under visible light," in *Proceedings of the Eco-Energy and Materials Science and Engineering Symposium*, vol. 9, pp. 509–514, 2011.

[4] R. Ahmadkhani and A. Habibi-Yangjeh, "Facile ultrasonic-assisted preparation of Fe_3O_4/Ag_3VO_4 nanocomposites as magnetically recoverable visible-light-driven photocatalysts with considerable activity," *Journal of the Iranian Chemical Society*, vol. 14, no. 4, pp. 863–872, 2017.

[5] H. Zhu, B. Yang, J. Xu et al., "Construction of Z-scheme type CdS-Au-TiO_2 hollow nanorod arrays with enhanced photocatalytic activity," *Applied Catalysis B*, vol. 90, no. 3-4, pp. 463–469, 2009.

[6] Q. Gu, H. Zhuang, J. Long et al., "Enhanced Hydrogen production over C-doped CdO photocatalyst in Na_2S/Na_2SO_3 solution under visible light irradiation," *International Journal of Photoenergy*, vol. 2012, Article ID 857345, 7 pages, 2012.

[7] S. Peng, A. Ran, Z. Wu, and Y. Li, "Enhanced photocatalytic hydrogen evolution under visible light over Cd x Zn_{1-x} S solid solution by ruthenium doping," *Reaction Kinetics, Mechanisms and Catalysis*, vol. 107, no. 1, pp. 105–113, 2012.

[8] Y. M. Yuxin and Y. I. Mixajlov, *Chemistry of Bismuth Compounds and Materials*, Iizdatelstvo SO RAN, Novosibirsk, Russia, 2001.

[9] A. Slikkerveer and F. de Wolff, "Toxicity of bismuth and its compounds," *Toxicology Methods*, no. 2, pp. 439–454, 1996.

[10] C. Wang, Z. Zhao, B. Luo, M. Fu, and F. Dong, "Tuning the morphological structure and photocatalytic activity of nitrogen-doped $(BiO)_2CO_3$ by the hydrothermal temperature, corporation," *Journal of Nanomaterials*, vol. 2014, Article ID 192797, 10 pages, 2014.

[11] X. Dong, W. Zhang, W. Cui et al., "Pt Quantum pots deposited on N-doped $(BiO)_2CO_3$: enhanced visible light photocatalytic no removal and reaction pathway," *Catalysis Science & Technology*, vol. 7, no. 6, pp. 1324–1332, 2017.

[12] Y. J. Wang, Y. M. He, T. T. Li, J. Cai, M. F. Luo, and L. H. Zhao, "Photocatalytic degradation of methylene blue on $CaBi_6O_{10}/Bi_2O_3$ composites under visible-light," *Chemical Engineering Journal*, vol. 189–190, pp. 473–481, 2012.

[13] P. Kanlaya, N. Wetchakun, W. Kangwansupamonkon, K. Ounnunkad, B. Inceesungvorn, and S. Phanichphant, "Photocatalytic mineralization of organic acids over visible-light-driven Au/$BiVO_4$ photocatalyst," *International Journal of Photoenergy*, vol. 2013, Article ID 943256, 7 pages, 2013.

[14] A. V. Shtareva, D. S. Starev, K. S. Makarevich, and M. B. Pereginyak, "Sposob polucheniya fotokatalizatora na osnove vismutata shhelochnozemelnogo metalla i sposob ochistki vody ot organicheskix zagryaznitelej fotokatalizatorom," A method for producing a photocatalyst based on an

alkaline earth metal bismuthate and a method for purifying water from organic contaminants with a photocatalyst, Patent RUS, no. 2595343, 2014.

[15] R. S. Roth, C. J. Rawn, B. P. Burton, and F. Beech, "Beech phase equilibria and crystal chemistry in portions of the system SrO-CaO-Bi_2O_3-CuO, part II—the system SrO-Bi_2O_3-CuO," *Journal of Research of the National Institute of Standards and Technology*, vol. 95, no. 3, pp. 291–335, 1990.

[16] Y. V. Karyakin and I. I. Angelov, "Pure chemicals," *M: Ximiya*, p. 408, 1974.

[17] A. V. Zajtsev, O. I. Kaminsky, K. S. Makarevich, and S. A. Pjachin, "Avtomatizirovannyj kompleks dlya issledovaniya sorbcionnoj i fotokataliticheskoj aktivnosti s obedinennoj reakcionnoj i izmeritelnoj chastyu," (The automated complex for examination of getter and photocatalytic activity with the incorporated reactionary and measuring part), Sbornik nauchnyx soobshhenij (DVGUPS), no. 22, pp. 57–63, 2017.

[18] K. T. Jacoba and K. P. Jayadevan, "System Bi–Sr–O: synergistic measurements of thermodynamic properties using oxide and fluoride solid electrolytes," *Journal of Materials Research*, vol. 13, no. 7, pp. 1905–1918, 1998.

[19] A. H. Nethercot, "Prediction of fermi energies and photoelectric thresholds based on electronegativity concepts," *Physical Review Letters*, vol. 33, no. 18, pp. 1088–1091, 1974.